

# Applications of mRNA injections for analyzing cell lineage and asymmetric cell divisions during segmentation in the leech *Helobdella robusta*

Shaobing O. Zhang<sup>1</sup> and David A. Weisblat<sup>2,\*</sup>

<sup>1</sup>Graduate Group in Biophysics, LSA 385, University of California, Berkeley, CA 94720-3200, USA

<sup>2</sup>Department of Molecular and Cell Biology, LSA 385, University of California, Berkeley, CA 94720-3200, USA

\*Author for correspondence (e-mail: weisblat@berkeley.edu)

Accepted 23 February 2005

Development 132, 2103-2113

Published by The Company of Biologists 2005

doi:10.1242/dev.01802

## Summary

Synthetic mRNAs can be injected to achieve transient gene expression even for 'non-model' organisms in which genetic approaches are not feasible. Here, we have used this technique to express proteins that can serve as lineage tracers or reporters of cellular events in embryos of the glossiphoniid leech *Helobdella robusta* (phylum Annelida). As representatives of the proposed super-phylum *Lophotrochozoa*, glossiphoniid leeches are of interest for developmental and evolutionary comparisons. Their embryos are suitable for microinjection, but no genetic approaches are currently available. We have injected segmentation stem cells (teloblasts) with mRNAs encoding nuclear localized green fluorescent protein (nGFP) and its spectral variants, and have used tandem injections of nGFP mRNA followed by antisense morpholino oligomer (AS MO), to label single blast cell clones. These techniques permit high resolution cell lineage tracing in living

embryos. We have applied them to the primary neurogenic (N) lineage, in which alternate segmental founder cells (nf and ns blast cells) contribute distinct sets of progeny to the segmental ganglia. The nf and ns blast cell clones exhibit strikingly different cell division patterns: the increase in cell number within the nf clone is roughly linear, while that in the ns clone is almost exponential. To analyze spindle dynamics in the asymmetric divisions of individual blast cells, we have injected teloblasts with mRNA encoding a tau::GFP fusion protein. Our results show that the asymmetric divisions of n blast cells result from a posterior shift of both the spindle within the cell and the midbody within the mitotic spindle, with differential regulation of these processes between nf and ns.

Key words: Leech, mRNA injection, Cell lineage, Asymmetric division, GFP

## Introduction

Embryos of the glossiphoniid leech *Helobdella robusta* are relatively large, hardy and experimentally tractable. They are therefore useful for comparative studies of segmentation among phylogenetically distant taxa (Annelida, Chordata, Arthropoda).

In contrast to known vertebrate and arthropod systems, segmentation in *Helobdella* proceeds via stereotyped lineages, beginning with the first mitosis and continuing, so far as is known, through the formation of terminally differentiated, segmentally iterated cells (Whitman, 1878; Zackson, 1984; Kramer and Weisblat, 1985; Weisblat and Shankland, 1985; Bissen and Weisblat, 1989; Braun and Stent, 1989; Shankland 1987; Muller et al., 1981). This assertion is qualified by the fact that no complete lineages for any definitive segmental progeny have been published.

In *Helobdella*, segmentation proceeds sequentially from a posterior growth zone comprising five bilateral pairs of large, identifiable segmentation stem cells (M, N, O, P and Q teloblasts; Fig. 1). Each teloblast lineage generates a stereotyped set of mesodermal (M) or ectodermal (N, O, P, Q) progeny to each segment, via coherent columns of segmental founder cells (blast cells). Previous studies have revealed two

major differences at the cellular level between the segmentation processes in leeches and arthropods. First, compartments as defined for *Drosophila* (Garcia-Bellido et al., 1973) are not observed in *Helobdella*. Instead, the stereotyped clones arising from individual blast cells interdigitate both mediolaterally (between lineages) and anteroposteriorly (within given lineages, across segment boundaries) (Weisblat and Shankland, 1985). Second, clitellate annelid embryos exhibit two distinct modes of stem cell divisions: the M, O and P teloblasts follow a parental mode in which each blast cell generates an entire segmental complement of progeny for its lineage; but the N and Q teloblasts follow a grandparental mode, in which two blast cells are required to generate each segmental complement, and the blast cells within each column follow distinct fates in exact alternation (Weisblat et al., 1980; Weisblat and Shankland, 1985; Storey, 1989; Arai et al., 2001).

Each teloblast lineage exhibits a specific pattern of blast cell division patterns (Zackson, 1984; Bissen and Weisblat, 1989). For the N and Q lineages, this includes differences in the timing and symmetry of the early divisions of alternating blast cells, designated as nf and ns, qf and qs, respectively. An intriguing issue is whether these cells assume distinct fates at birth or as a result of interactions within the n and q bandlets. Segment-

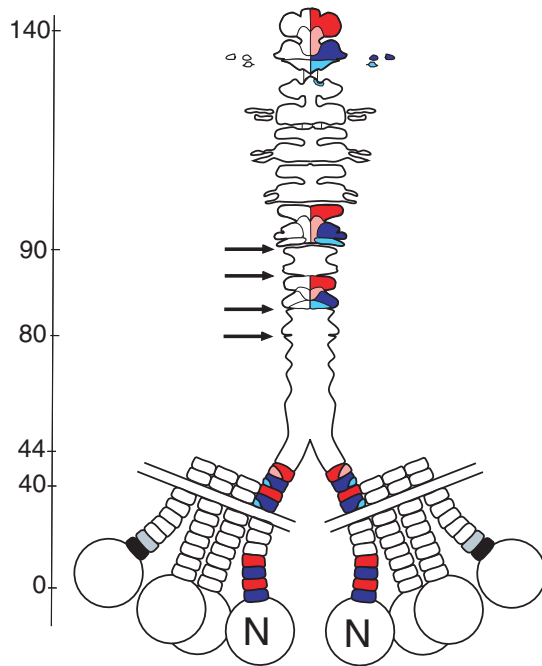


**Fig. 1.** Events in the N lineage leading to gangliogenesis in *H. robusta*. Cleavage yields an embryo with a posterior growth zone of five bilateral pairs of segmentation stem cells (teloblasts); only the four pairs of ectoteloblasts are shown here. Ignoring gastrulation, segments arise in anteroposterior progression along the ventral midline by the stereotyped divisions of columns of segmental founder cells (blast cell bandlets). In the N (and Q lineages), clones of two successive blast cells, designated ns (red) and nf (blue) contribute distinct sets of progeny to each segment. Because blast cells of each type execute a stereotyped pattern of cell division relative to the time of their birth from the parent teloblast, events in the generic nf and ns lineages can be designated as occurring at a specific 'clonal age' (cl.ag.), as indicated on the time line on the left. Primary n blast cells divide unequally, producing larger anterior (nf.a, dark blue; ns.a, red) and smaller posterior (nf.p, light blue; ns.p, pink) daughter cells (40 and 44 hours cl.ag., respectively). Transverse fissures (arrows) separate nf.p clones (light blue) from ns.a clones (red) dividing the bandlets into discrete ganglionic primordia (85-95 hours cl.ag.). Anterior is upwards in all figures unless otherwise noted.

specific identities of blast cells in the M and O lineages are assigned long before the primary blast cells divide (Martindale and Shankland, 1990; Gleizer and Stent, 1993; Nardelli-Haeffliger et al., 1994), and results correlating the nf and ns fates with subtle differences in the teloblast cell cycle support the grandparental mode model (Bissen and Weisblat, 1987). The overt differences between the nf and ns blast cells in the timing and symmetry of their initial mitoses provide a point of entry to exploring how nf and ns fates are assigned.

Microinjection of fluorescent dextrans (Gimlich and Braun, 1985) has been the technique of choice for analyzing cell lineages in *Helobdella*, but it becomes difficult to distinguish individual cells in the marked clones as the cells increase in number and decrease in size, especially when they lie adjacent to one another. More recently, diverse applications employing fluorescent proteins (GFP, YFP, CFP and DsRed; designated collectively here as XFPs) have been used to label specific cells

in vivo (Tsien, 1998; Lippincott-Schwartz and Patterson, 2003). These fluorescent proteins can be fused to target genes, allowing inferences to be drawn about their expression and localization in live embryos of various sorts (Chalfie et al., 1994; Lee and Luo, 1999; Amsterdam et al., 1995; Feng et al., 2000).

Here, we have injected mRNAs encoding various XFP constructs in a combination of lineage tracing and reporter construct technologies, focusing on the primary neurogenic (N teloblast) lineage in *H. robusta*. We found that these mRNAs meet all the criteria for being microinjectable lineage tracers. In particular, the spatially restricted fluorescence of nuclearly localized XFP (nXFP) enabled us to extend our knowledge of the nf and ns blast cell lineages and revealed dramatic differences between them. We have also characterized the degree of asymmetry of the primary nf and ns blast cell divisions by using nXFP fluorescence to measure the nuclear volumes of the daughter cells. To follow the spindle dynamics of dividing nf and ns blast cells, we injected mRNA encoding tau::GFP. The spindle dynamics in the dividing ns and nf cells showed both similarities and differences to those in the asymmetric divisions of the *C. elegans* zygote and *Drosophila* neuroblasts.

## Materials and methods

### Embryos

Embryos were obtained from a laboratory-cultured strain provisionally identified as an Austin (Texas) strain of *Helobdella robusta* (Seaver and Shankland, 2000; Kuo and Shankland, 2004). Embryos were cultured in HL saline and maintained at 23°C. Staging and cell nomenclature are as defined previously (Weisblat and Huang, 2001) for the holotypic strain of *H. robusta* collected in Sacramento (California) (Shankland et al., 1992), but the strains differ in the relative rates at which they progress through certain stages (S.O.Z. and D.A.W., unpublished), and in the sequences of various genes that have been studied (A. E. Bely, personal communication). In *Helobdella*, segments arise from seven distinct sublineages, founded by m, nf, ns, o, p, qf and qs blast cells (see Fig. 1 for details).

### Plasmid constructs, mRNA synthesis and mRNA injection

eGFP mRNA was transcribed in vitro from linearized pCS2P-eGFP-X/P plasmid. Nuclear localized GFP and  $\beta$ -galactosidase (nGFP and nLacZ) and tau::GFP mRNAs were transcribed from pCS2P-nls-eGFP, pCS2-nls- $\beta$ gal and pCS2-tau-GFP plasmids, respectively. To make nuclear localized versions of other fluorescent proteins, plasmids pECFP-N1, pEYFP-N1 and pDsRed2-N1 (Clontech) were used as templates (details available on request). RNA was injected from standard glass pipets treated to avoid RNase contamination (details available upon request). The concentration of mRNAs in the needle are 0.4  $\mu$ g/ $\mu$ l (GFP, nGFP, nCFP, nYFP, nRFP, tau::GFP) or 0.1  $\mu$ g/ $\mu$ l (nLacZ), either with or without 5  $\mu$ g/ $\mu$ l rhodamine dextran amine (RDA, Molecular Probes), the final concentration of mRNAs in the teloblast was estimated to be 4 ng/ $\mu$ l or 1 ng/ $\mu$ l, as the injected volume is estimated to be 1% of that of the N teloblast.

### Morpholino injection

Antisense morpholino oligomer (AS MO, Gene Tools) complementary to the start codon and seven downstream codons of nGFP mRNA, designated as AS-nGFP MO (5'-CCTTACGCTTCTTCTTTG-GAGCCAT-3'; anti-start codon underlined), was injected at a concentration of 0.1 mM in the needle (1  $\mu$ M in the teloblast) if not otherwise indicated. AS-nGFP MO was used as a 4-mismatch control morpholino to nCFP and nYFP mRNA, which are similar in this

region (5'-ATGGCaCCgAAGAAGAAGaGgAAGG-3'; mismatches are in lowercase and the start codon is underlined). The sequence of AS-nLacZ MO is 5'-TACGCTTCTTCTTTGGAGCAGTCAT-3' with the anti-start codon underlined. Injections procedures were as for mRNA injection. At least 20 embryos were injected for each experimental time point and all experiments were performed in triplicate at minimum.

### Time-lapse fluorescence microscopy and imaging processing

Injected embryos were allowed to develop to desired stages, mounted in HL saline then examined and photographed using a Nikon E800 epifluorescence microscope equipped with a cooled CCD camera (Princeton Instruments), controlled by Metamorph software (UIC). Confocal time-lapse images were obtained under Zeiss 510 Axioplan microscope at a time interval of 1 hour (40-60 planes at 0.5  $\mu$ m steps, using 63 $\times$  objective-water immersion NA 0.90). To image segmental ganglia, stage 10 embryos were fixed (4% formaldehyde in 1 $\times$  PBS), washed (1 $\times$  PBS), then dissected. The germinal plates were mounted and observed in 1 $\times$  PBS.

Confocal image stacks of ns/nf clones and stage 9-10 ganglia were deconvolved and reconstructed using Imaris 4.0 (Bitplane AG), or Volocity 3.0 (Improvision); nuclei were annotated and measured in Volocity. Epifluorescence images were deconvolved (2-D), then reconstructed in Metamorph. Images were exported as movies and single snapshots, and further processed with Photoshop 5.0 (Adobe) to prepare figures. Spindle images were processed and converted into time-lapse movies using Metamorph.

### In situ hybridization, X-gal staining and Hoechst staining

Antisense GFP probe was made using T7 MEGAscript kit (Ambion) and hybridizations were as previously described (Song et al., 2002). X-gal staining was as previously described (Liu et al., 1998), or as modified from a protocol in *Xenopus* (Sive et al., 2000) (details upon request). Embryos were counterstained and mounted for observations as previously described (Shain et al., 2000).

## Results

### Nuclear localized fluorescent proteins as lineage tracers

For cell lineage studies using fluorescently labeled dextrans or GFP, the cytoplasmic distribution of the fluorescence makes it hard to distinguish individual cells in the germinal bands and germinal plate, especially in lineages where small cells are closely apposed (Bissen and Weisblat, 1989; Huang et al., 2002). To circumvent these problems, we tested mRNA encoding nuclear localized GFP (nGFP) as a cell lineage tracer in living embryos, and found that it meets the three criteria required of any microinjected lineage tracer: (1) confinement to the clone of the injected cell; (2) stability and detectability during extended periods of development; and (3) not perturbing normal development. This last criterion was of particular concern given the nuclear localization of the nGFP; it was easy to imagine that it might perturb the normal lineages.

N teloblasts in stage 7 embryos (~33 hours AZD) were injected with RDA and nGFP mRNA. After ~48 hours of subsequent development, the pattern of nGFP-labeled nuclei was as expected from previous studies (Zackson, 1984; Bissen and Weisblat, 1989) (not shown). In other experiments, we allowed injected embryos to develop for 143 hours post-injection. As at earlier stages, the distribution of marked cells was indistinguishable from when teloblasts were with injected with RDA only. The nGFP was still readily detectable, and cell

nuclei in the labeled clone were observed with excellent resolution. We counted ~100 nuclei in the anteriormost labeled hemiganglion and the N-derived peripheral neurons (nz1-3) were observed at their stereotyped positions (Fig. 2A,B). In a third set of embryos, both N and P teloblasts were injected with nGFP mRNA and examined at ~100 hours post-injection; neural precursor cells had migrated medially from the p bandlet (Fig. 2C) as reported previously for *Theromyzon* (Torrence and Stuart, 1986) and *Helobdella* (Braun and Stent, 1989). Thus, nGFP showed excellent perdurance and did not noticeably perturb development (Fig. 2D).

Spectral variants of GFP (collectively designated XFPs) are

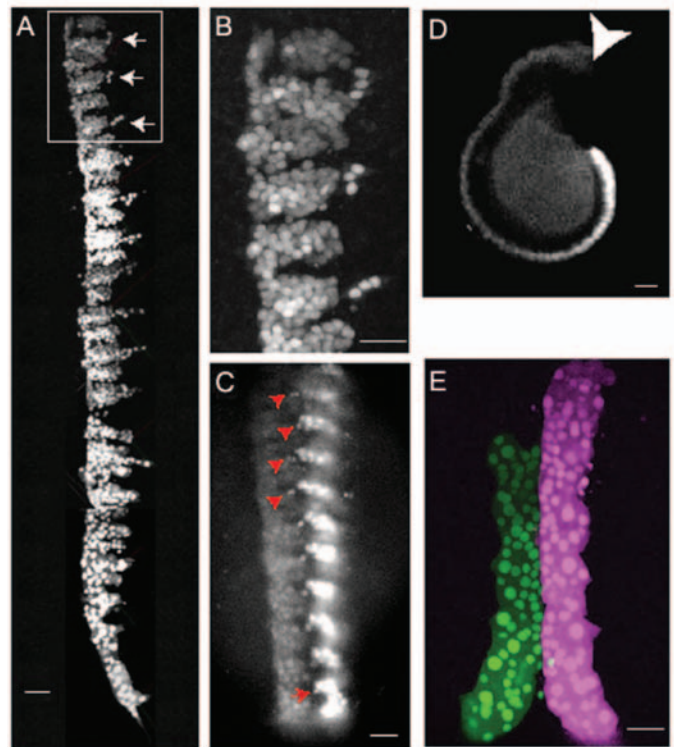


**Fig. 2.** nXFPs as lineage tracers in *Helobdella*. (A) Photomontage made from stacks of confocal images (processed by Imaris, Bitplane) showing a ventral view (midline to left) of a stage 10 embryo, 140 hours after the left N teloblast had been injected with nGFP mRNA. nGFP labeled nuclei occupy the anterior and posterior lobes of N-derived ganglionic neurons and the three peripheral neurons lying just outside the posterior (nf-derived) lobe (arrows). (B) Higher magnification view of the boxed region in A. (C) Epifluorescence images of the germinal plate of a late stage 8 embryo (ventral midline towards the left) about 100 hours after the left N and P teloblasts were injected with nGFP mRNA. The N and P lineages can be distinguished by a difference in fluorescence intensity, reflecting differences in the amount of mRNA injected into the parent teloblasts. The temporal gradient of development is evident in the progress of migrating neurons (arrowheads) which originate from a single cell at the medial edge of the p blast cell clone (arrow). (D) Side view of an early stage 10 embryo, 150 hours after the left N teloblast had been injected with nGFP mRNA shows an anterior (arrowhead) to posterior gradient of GFP intensity. (E) Pseudocolored image (confocal stack) showing a ventral view of a live mid stage 8 embryo, 83 hours after one N teloblast had been injected at stage 7 with nCFP mRNA and the other with nYFP mRNA 3 hours later (nCFP, purple; nYFP, green). Scale bar: 20  $\mu$ m.

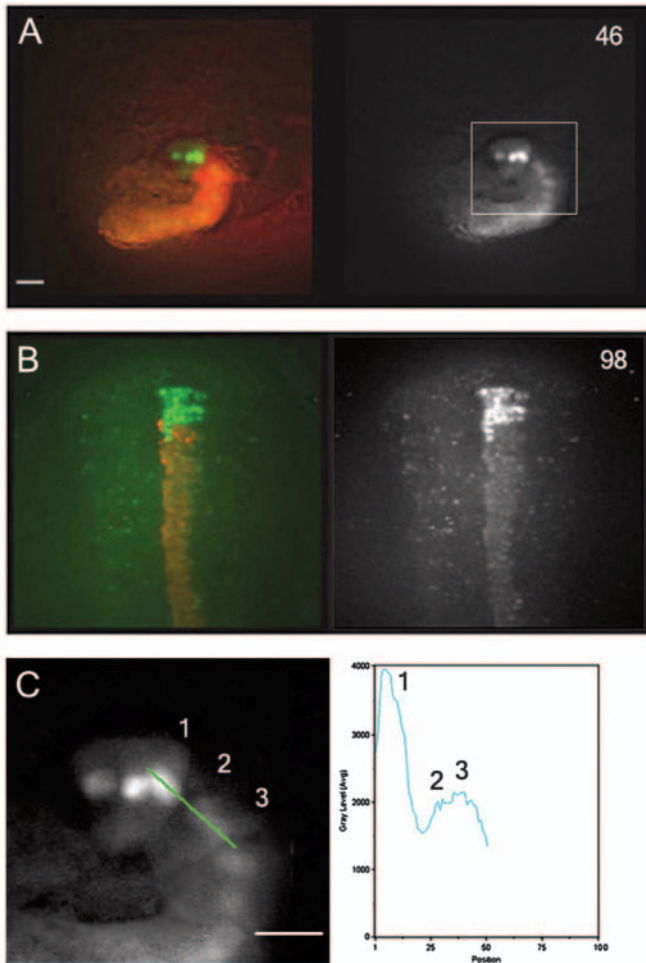


**Fig. 3.** AS MO knockdown of injected mRNA expression. (A,B) N teloblasts were injected at stage 6 with nGFP mRNA, 3 hours later with a mixture of fluorescent dextran (RDA) and antisense morpholino oligomer (AS MO), and then imaged after another 46 and 98 hours. The left side of each panel shows the combined RDA (red) and nGFP (green), and the right side shows nGFP only, revealing the decrease in nGFP fluorescence in clones produced after the AS MO injection. In these experiments, two or three blast cells were produced between the first and second injections. (C) Enlarged view of the embryo shown in A; fluorescence intensity was measured along the line shown crossing blast cell nuclei produced before and after the AS MO injection and plotted on the right. Scale bar: 10  $\mu$ m.

widely used (Lippincott-Schwartz and Patterson, 2003). We made and tested several XFPs for use in multi-label lineage tracing (see Materials and methods for details). Injection of mRNAs for nCFP and nYFP produced strong, nuclear-localized fluorescence (Fig. 2E), with the same perdurance and benignity as nGFP; nRFP, however, showed a much shorter half-life (data not shown), so the version of nRFP used here is not useful for long term lineage tracing in *Helobdella*.

To further refine the mRNA injections technique in *Helobdella*, we used it to test the efficacy of antisense knockdown reagents. RNAi did not yield reproducible knockdowns (data not shown), but antisense morpholino oligomer (AS MO) injections did. For this purpose, teloblasts were injected with nGFP mRNA and then after 3 hours, with AS MO complementary to 5' sequence of nGFP mRNA (AS-

nGFP MO; see Materials and methods for details). We observed a significant and long-lasting knockdown of nGFP fluorescence in the primary blast cells and their clones that received AS-nGFP MO, relative to the cells produced prior to the second injection (Fig. 3A,B); in similar experiments, AS MO knockdown of nLacZ expression was also obtained (data not shown). Using quantitative fluorescence measurements, we estimate a knockdown of about 50% (Fig. 3C). No knockdown occurred when the target mRNA bore a mismatched target sequence or when the second injection comprised RDA only (data not shown).

### Distribution and perdurance of injected mRNA and protein

We routinely observed a gradient of increasing GFP fluorescence within the progeny of the injected teloblasts (Fig. 2A,D,E). The nGFP fluorescence must be determined by a complex dynamic involving nGFP mRNA and protein. To examine the stability and distribution of the injected mRNA, N teloblasts were injected with nGFP mRNA in stage 7 embryos (33 hours AZD), which were then fixed at 1-120 hours post-injection, then processed in parallel to insure comparable in situ staining.

Examining these embryos (Fig. 4), we concluded that the injected mRNA diffused throughout the injected teloblast and was readily passed on to the primary blast cell progeny. The nGFP mRNA degraded more quickly within the blast cell clones than within the teloblast and primary blast cells, however; n blast cells produced after the injection stained

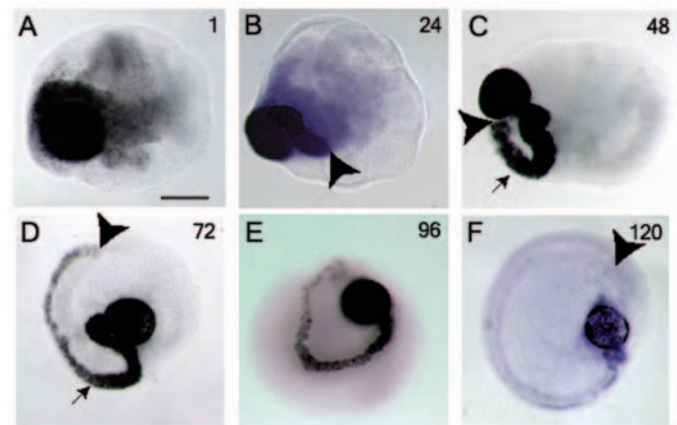


**Fig. 4.** Distribution and perdurance of injected mRNA. N teloblasts in stage 7 embryos were injected with nGFP mRNA. The embryos were fixed at times ranging from 1-120 hours post-injection, then processed in parallel for in situ hybridization. Arrowheads indicate the position of the first labeled clone, where visible. (A-D) Animal pole views of embryos fixed 1-72 hours after injection. The teloblast and relatively young blast cells (arrowhead in B) stained intensely, but a significant decline in staining was apparent in blast cell clones that had undergone their first mitosis (arrow in C,D). (E) Prospective posterior view of an embryo fixed 96 hours after injection. Although the teloblast still stained very intensely, the first labeled clone (not visible in this view) was barely visible. (F) By 120 hours after injection (side view), staining in the teloblast was clearly reduced, but still clear. By contrast, nGFP mRNA was no longer detectable in the first labeled clone under these conditions (arrowhead indicates the estimated position of the first labeled clone; compare with Fig. 2A,D). Scale bar: 100  $\mu$ m.

intensely during the first 24 hours post-injection, at which time they have not yet divided, but by 72 hours post-injection the mRNA was barely detectable within the equivalent cell clone. Comparisons with RDA injections indicate that this reflects mRNA breakdown and not dilution (data not shown). At 120 hours post-injection, nGFP mRNA was readily detected in the injected teloblast and supernumerary blast cells and faintly in the most posterior segments, but not in any of the anterior segmental progeny. Thus, the *in situ* signal results indicate the perdurance of translatable transcripts in blast cell clones until ~72 hours cl.ag. Finally, nGFP protein could be readily detected throughout the germinal plate for as long as 145 hours post-injection, i.e. ~3 days after no nGFP mRNA could be detected (compare Fig. 2D with Fig. 4F). We conclude that the anteroposterior gradient of nGFP reflects gradually increasing levels of nGFP protein and decreasing levels of nGFP mRNA inherited by successive blast cells from the parent teloblast, coupled with declining levels of residual nGFP protein in older blast cell clones, from which the mRNA has been degraded. Similar gradients of expressed protein were seen with all the synthetic mRNAs used (data not shown).

#### Cell lineage analysis by nGFP mRNA microinjection

We used the mRNA techniques described above to elucidate cell division patterns in the N lineage. Knowing the complete lineage of the *Helobdella* embryo is a long term goal, but here we focused on differences between the ns and nf blast cell lineages, and resolving uncertainties regarding the fates of the early progeny of the N teloblasts.

Ganglionic primordia separate as the nf.p clone in one neuromere delaminates from the ns.a clone in the next (fissure formation) (Shain et al., 1998). To identify differences between the nf and ns clones, we sought to compare the lineages leading from the continuous columns of primary blast cells to the separation of ganglionic primordia. Fissure formation occurs between ~45-50 hours cl.ag. in *Theromyzon rude* (Shain et al., 1998), corresponding to ~85-95 hours cl.ag. in the Austin strain of *H. robusta* (Fig. 1).

For this purpose, tandem injections ~90 minutes apart were used to uniquely label single blast cell clones (Zackson, 1982). Labeled embryos were then examined by time-lapse confocal microscopy, beginning at 58 hours cl.ag., by which time the first labeled clone (an ns clone) contained two or three cells (Fig. 5A). To identify the limits within which photo-damage did not perturb development, we compared the patterns of labeled nuclei in embryos subjected to various illumination paradigms with those in equivalent embryos that were imaged only at the end of the experiment. We found that sampling embryos at a 1 hour time interval was sufficient to capture cell divisions and movements in the N lineage during the period of interest, and that after a 12 hour observation period, the pattern of labeled nuclei was as in an unirradiated sibling embryo (Fig. 5A). These results suggested that cell divisions had occurred normally during this period in the imaged embryos. However, imaging periods greater than 12 hours often resulted in arrested cell division, so to follow further events in the nf and ns lineages, we undertook multiple overlapping time-lapse imaging experiments covering 40-86 hours cl.ag. for the ns clone and 40-82 hours cl.ag. for the nf clone.

For this, the N teloblast was injected with nGFP mRNA at the beginning of stage 7. Under this protocol, the first labeled

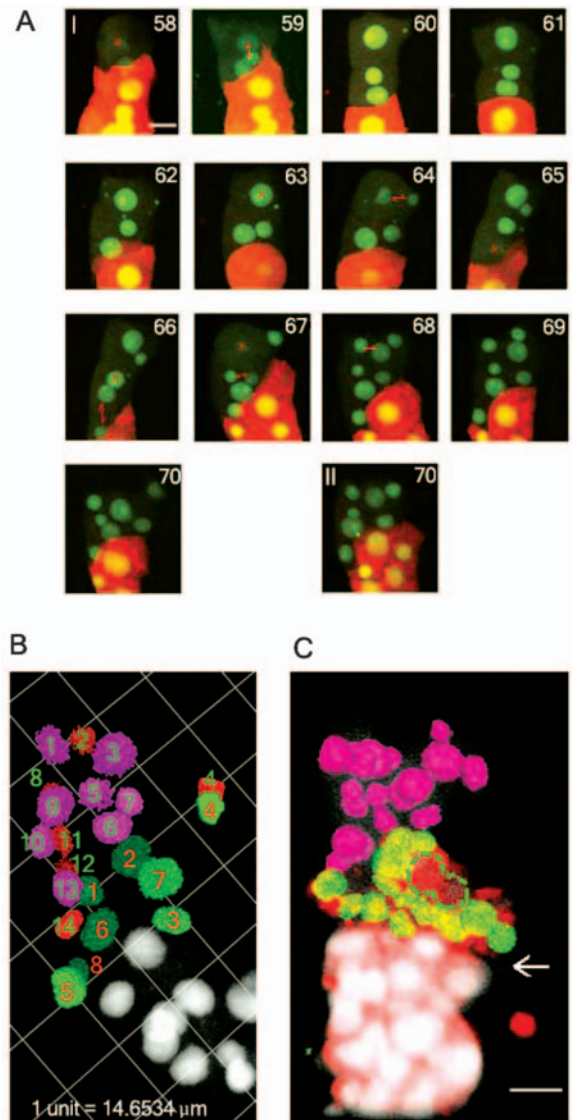


**Fig. 5.** Application of nGFP mRNA injections to analysis of the N lineage. (A) Time series showing the anterior portion of an n bandlet; one ns blast cell was uniquely labeled by tandem injections of the parent teloblast, first with nGFP mRNA and then, after one blast cell was born, with RDA. Beginning 58 hours after the first injection (I, 58-70), the uniquely labeled clone was imaged hourly for 12 hours. During this time, the clone increased from two cells to seven; a similar pattern of nuclei was observed in a sibling embryo imaged only at 70 hours cl.ag. (II, 70). (B) Reconstruction of an embryo injected as in A at 86 hours cl.ag. In the first (ns) labeled clone, superficial nuclei are pseudocolored lavender and deep nuclei (2, 4, 8, 11, 12, 14) are red (8 and 12 are obscured by overlying nuclei). In the next (nf) clone, nuclei are pseudocolored green. Those in more posterior clones appear white. The numbers over the nuclei of the ns and nf clones correspond to cells in the lineage trees in Fig. 6A and B, respectively. (C) Three-dimensional reconstruction of a similar embryo with the ns clone at 90 hours cl.ag. The ns clone (lavender) now has 18 nuclei; the posterior nf clone (green) has 18 interphase nuclei and one in mitosis (broken outline); the exact identities of these cells remain to be determined. In this panel, the cytoplasmic RDA fluorescence is shown in red surrounding nuclei in the nf and more posterior (white) clones, so that the elongating fissure between prospective ganglionic primordia is visible (arrow); midline towards left in B and C. Scale bar: 10  $\mu$ m.

clone was invariably the ns clone contributing to the fourth segmental neuromere of the rostral ganglionic mass (neuromere R4). Unfortunately, our observations ended ~4 hours and several cell divisions prior to the appearance of the transverse fissure separating neuromeres R4 and M1 (Fig. 5B,C). The ns and nf blast cell clones had increased to 14 and 8 cells, respectively, by this time, including one dying cell in each clone (revealed by nuclear morphology and cell fragmentation; data not shown; Fig. 5B, Fig. 6); apoptoses of unknown lineage within the germinal bands had previously been reported (Tsubokawa and Wedeen, 1999). Three results of this study were as follows.

First, the lineages were consistent; the orientation and relative order of mitoses was preserved within each clone, although the timing varied up to several hours between embryos. This could reflect temperature differences between experiments. Cell movements, judged by changes in the relative positions of nuclei, were also stereotyped.

Second, many divisions exhibited stereotyped asymmetries, as judged by the relative volumes of the nuclei of the daughter cells (Fig. 7). Asymmetric divisions of the nf and ns blast cells have been described qualitatively (Bissen and Weisblat, 1989; Song et al., 2002). Here, we measured the nuclear volume ratios for the daughter cell pairs of 26 ns and 31 nf divisions. There was no overlap between the ratios for ns and nf divisions and little variation within each class of n blast cells (Fig. 7B), despite the fact that the exact clonal age and position of the dividing cells varied significantly between embryos. We conclude that the differentially asymmetric ns and nf divisions reflect inherent differences between the two blast cell types. Asymmetric cell divisions occurred throughout the regions of the ns and nf lineages studied here. After each asymmetric division, the smaller daughter cell (as judged by nuclear volume) invariably had a longer cell cycle than its sister, but there was not a strict correlation between nuclear volume and cell cycle duration overall (data not shown).

Third, the ns clone underwent more divisions and fewer cell rearrangements than nf during the period under investigation. Cell divisions within the nf clone were largely confined to the successive anterior daughter cells, as if this cell were serving as a neuroblast, and nf.p did not divide at all. By contrast, cell divisions occurred throughout the ns sublineage, which thus contained roughly twice as many cells as the nf clone by the end of the period (Fig. 6). Similar results were obtained for the *H. robusta* strain isolated from Sacramento (California) (F. Z. Huang, personal

communication). These experiments focused on the ns and nf lineages in neuromere R4, but similarly structured clones occur throughout the labeled bandlet, indicating that other ns and nf clones undergo similar patterns of early divisions.

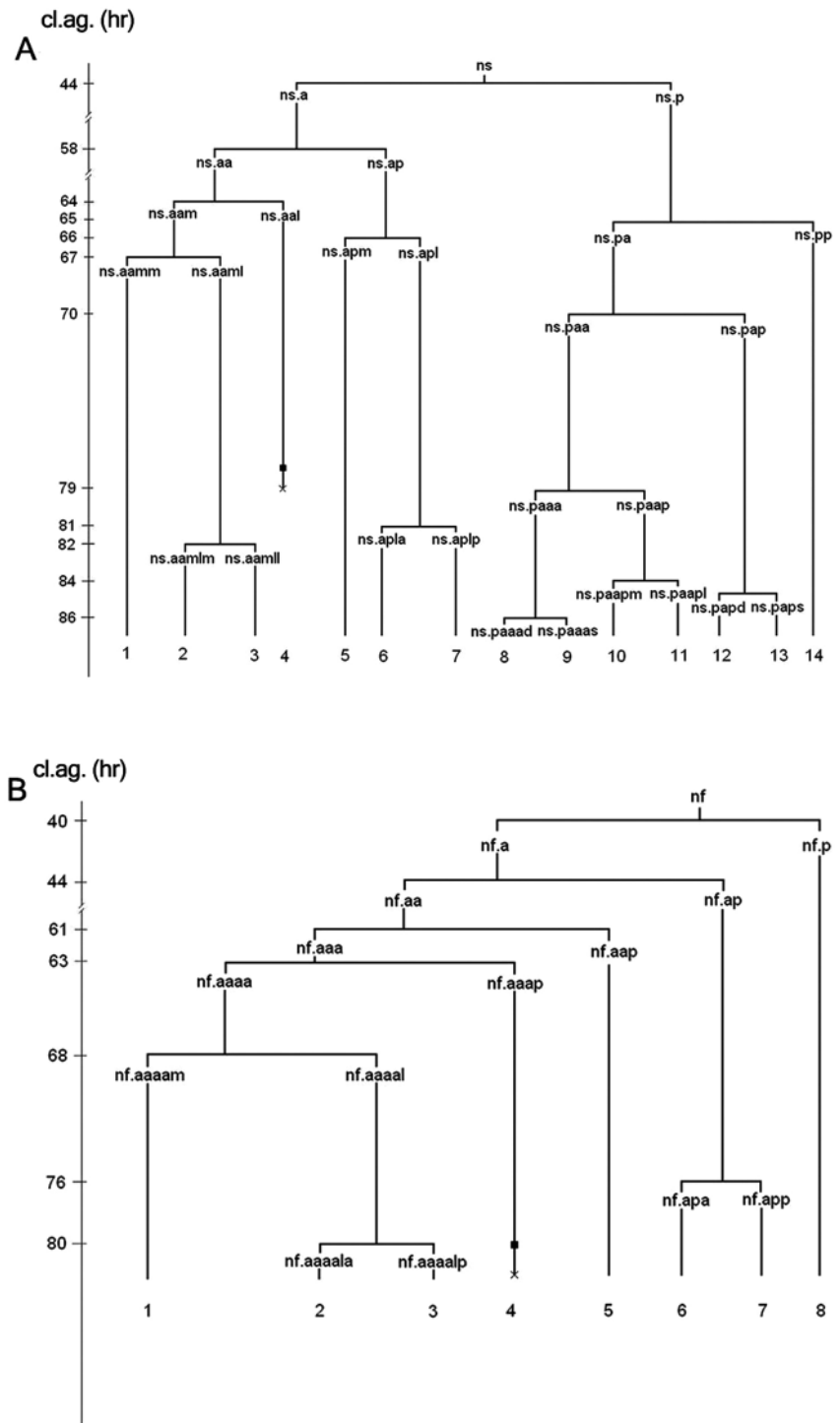


**Fig. 6.** Diagram of the early ns (A) and nf (B) blast cell lineages (non-linear time scale). Cell nomenclature is adapted from *C. elegans* as described previously (Huang et al., 2002). anterior, a; posterior, p; medial, m; lateral, l; superficial, s; deep, d. The cl.ag. given for each division represents the average of observations drawn from three to five specimens in each case. Numbers correspond to the cells in Fig. 5B.

### Non-standard N teloblast progeny

The N teloblasts also contribute two sets of non-segmental cells to the anterior micromere cap (Smith and Weisblat, 1994). One

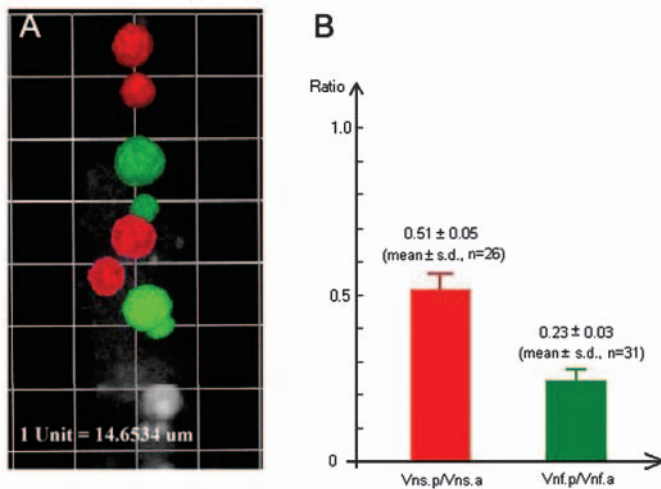


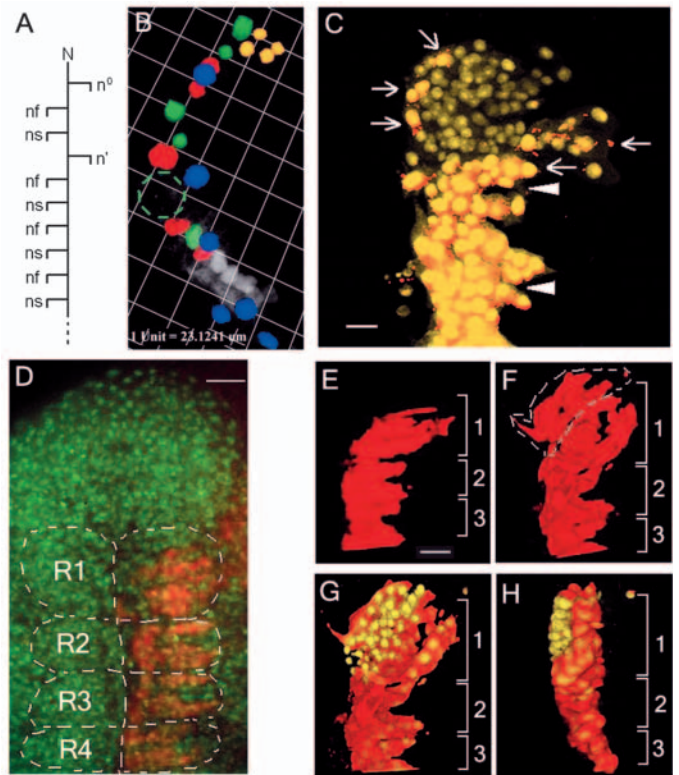
**Fig. 7.** Asymmetric blast cell mitoses: nuclear volume ratios of nf and ns progeny. (A) Pseudocolored 3-D reconstruction of an nGFP labeled n bandlet, showing two two-cell ns blast cell clones (red) and two two-cell nf blast cell clones (green). (B) Graph showing the ratio of the volumes (mean  $\pm$  s.d.) of cells like those shown in A.

**Fig. 8.** Early progeny of the N teloblast. (A) Lineage diagram showing divisions of the N teloblast. After its birth (stage 6a, ~22 hours AZD), the N teloblast divides every 90 minutes, generating a column of progeny that mostly follow the ns and nf (segmental founder cell) fates in exact alternation. But the fourth cell ( $n'$ ) contributes exclusively to the provisional epithelium, and the fates of cells born prior to  $n'$  were not known with certainty. (B) Pseudocolored 3D reconstruction of an nGFP-labeled n bandlet, 48 hours after the N teloblast was injected. The clone of the anteriormost cell contains four nuclei of equal size (yellow), unlike either nf or ns, so this is designated  $n^\circ$ . The three cells posterior to this have each divided once, in manner characteristic of the nf (green) or ns (red) clones. The nucleus in the sixth position (broken outline) has entered mitosis before the primary blast cell just ahead of it, also indicative of the nf (green) and ns (red) fates. By this time, the  $n'$  micromere clone contains six cells (blue), superficial to the bandlet. (C) Equivalent view of an older embryo, in which the N teloblast was re-injected with RDA after the birth of  $n^\circ$  (all nuclei are shown as yellow). By cl.ag. 96 hours, the  $n^\circ$  clone comprises 70–80 nuclei, distinguished by their smaller size and less intense fluorescence. Nuclei of the RDA labeled nf and ns blast cells are larger, brighter and surrounded by RDA fluorescence (red). The  $n^\circ$  clone is now flanked by cells derived from the anteriormost nf clone (arrows). Fissures (arrowheads) have formed between the posterior edges of the nf clones and the anterior edges of the adjacent ns clones. (D) Ventral view of the subesophageal ganglion and presegmental tissue of an embryo (~146 hours AZD) in which the left N teloblast was injected with RDA shortly before the birth of its first ns blast cell, i.e. after it had already produced cell  $n^\circ$  and the first nf blast cell. The embryo was counterstained with Hoechst 33258 (green). Broken outlines indicate the edges of the four neuromeres (R1–R4) in the subesophageal ganglion. Neuromere R1 contains the same complement of labeled neurons as neuromeres R2–R4, even though its anterior edge is unlabeled. (E) Pseudocolored 3D representation of the RDA-labeled cells in an embryo equivalent to that shown in D. (F–H) Pseudocolored images (processed as in C) of an embryo in which the N teloblast was injected with RDA after the birth of  $n^\circ$  (i.e. one cell cycle earlier than in D and E). The N teloblast had also been injected with nGFP mRNA prior to the birth of  $n^\circ$ . As a result, the  $n^\circ$  clone is labeled with nGFP only, and the first RDA-labeled clone is descended from the first nf cell. (F) Ventral view, comparable with E, showing only the RDA labeled cells; broken outline surrounds the first nf clone. (G) The same image as in F, with the addition of the  $n^\circ$ -derived nuclei (yellow). (H) Side view (ventral to left) of the image shown in G. Scale bar: 10  $\mu$ m.

is a clone of squamous epithelial cells derived from micromere  $n'$ , which arises from the N teloblast after it has already made three divisions (Sandig and Dohle, 1988; Bissen and Weisblat, 1989) (Fig. 8A). The other is a small domain of apparently columnar epithelial cells derived from one or more of the first three N teloblast progeny. To enable comparisons with lineage maps in other spiralian, we have resolved uncertainties regarding the fates of the cells produced prior to micromere  $n'$ .

Tandem injections were used to label uniquely the first cell produced by the N teloblast. We found that this cell follows neither the nf nor the ns fate, but instead contributes exclusively to the set of columnar epithelial cells. This cell (now designated  $n^\circ$ ) proliferates via equal and relatively rapid cell divisions. Its clone comprises four nuclei at cl.ag. 48 hours (Fig. 8B) and more than 80 cells by cl.ag. 96 hours (Fig. 8C). The second and third cells produced by the N teloblast follow the nf and ns fates, respectively, as judged by the timing and asymmetries of their first divisions (Fig. 8B), and the distribution of their progeny (Fig. 8C). As described previously, the fourth daughter of the N teloblast is micromere  $n'$ , then the N teloblast reverts to the production of alternating nf and ns blast cells, beginning with nf.

Finding that the anteriormost n blast cell is of the nf class is paradoxical because in standard neuromeres, the ns clone lies anterior to the nf clone (Fig. 1) (Bissen and Weisblat, 1987). The paradox is resolved by the realization that the anterior



neuromere of the subesophageal ganglion (R1) contains extra neurons compared with other neuromeres (Fig. 8D). These extra neurons arise from the *nf* clone (Fig. 8E,F), which could explain observations that the subesophageal ganglion contains more (N-derived) serotonergic neurons than expected from four fused standard neuromeres (Lent et al., 1991). Although we propose that it forms the anteroventral adhesive organ (Smith and Weisblat, 1994), the definitive fate of the *n*<sup>o</sup> clone remains to be determined. By 120 hours c.l.ag., the *n*<sup>o</sup>-derived cells lie immediately ventral to the first *nf* clone (Fig. 8G,H).

### Polarity and asymmetry of blast cell divisions

To examine the regulation of the asymmetric *n* blast cell divisions, we injected left N teloblasts with *tau::GFP* mRNA, then followed spindle dynamics in 26 *ns* and 18 *nf* divisions.

Mitosis took about 30 minutes for both *nf* and *ns* blast cells. No differences were observed until late in mitosis; in both *ns* and *nf*, spindle assembly was evidenced by increasing fluorescence intensity at the centrosomes (Fig. 9A, 00–04 minutes; Fig. 9B, 00–05 minutes). Centrosomes in the *n* blast cells had separated at several hours before the onset of mitosis (Fig. 9C), and usually retained an obliquely transverse orientation with respect to the AP axis of the *n* bandlet as cells rounded up for mitosis (Fig. 9A, 08 minutes; Fig. 9B, 05 minutes). In three of the divisions (1 *nf* and 2 *ns*), the centrosomes were already in an anteroposterior orientation prior to the onset of mitosis. No asymmetries were evident as the spindles began to rotate following nuclear breakdown (Fig. 9A, 12–20 minutes; Fig. 9B, 05–11 minutes).

Spindle rotation took 3–5 minutes and most spindles (22/26 *ns* and 16/18 *nf*) rotated counterclockwise, in contrast to the random directionality of spindle rotation in cell *P*<sub>0</sub> of *C. elegans* (Hyman, 1989). The blast cell spindle rotations proceeded without apparent hesitation or reversal of the spindle rotation, in apparent contrast to the jerky spindle rotation in cell *P*<sub>0</sub> of *C. elegans*, but this could result from the lower sampling rate required in our fluorescence imaging experiments to minimize photodamage. In several specimens, the spindle underwent back and forth movements between the anterior and posterior cortices after rotation (Fig. 9A, 20–24 minutes), as if there were competing pulling forces from the anterior and posterior cortices, as seen in *C. elegans* *P*<sub>0</sub> cell divisions (Grill et al., 2001).

Differences between *nf* and *ns* blast cells appeared late in

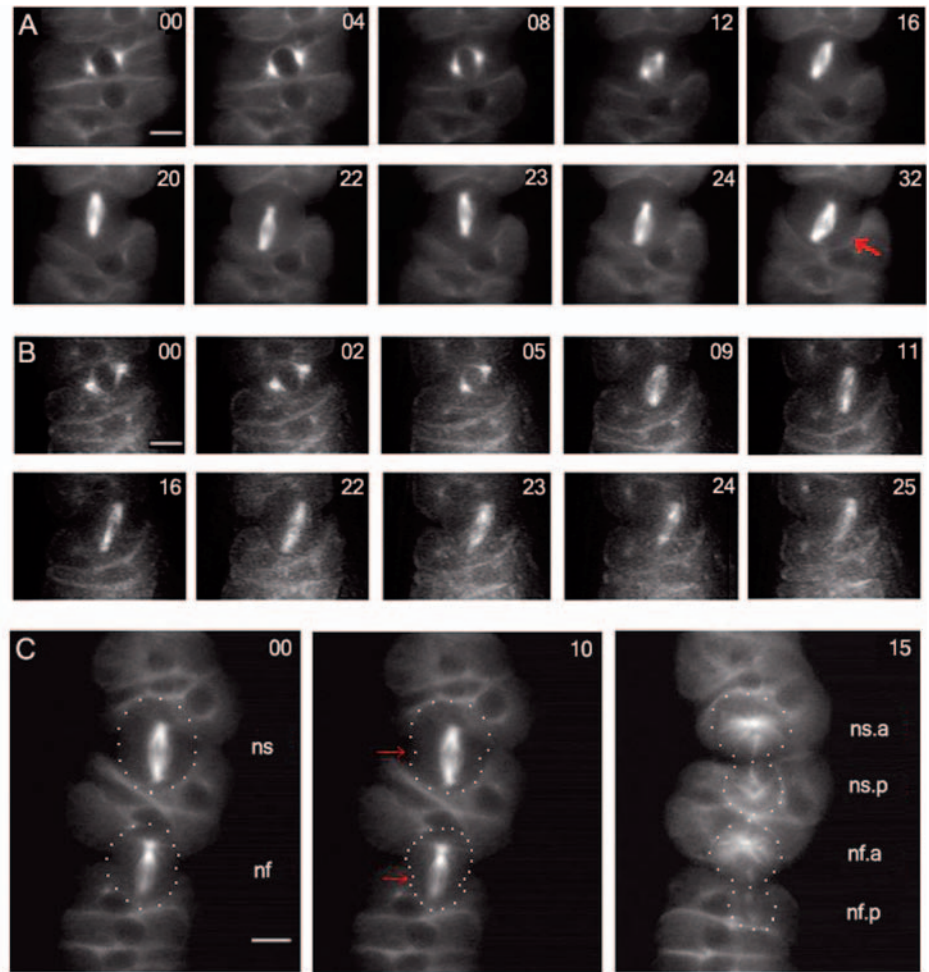


**Fig. 9.** Asymmetric mitoses of primary *nf* and *ns* blast cells: spindle dynamics. Time-lapse fluorescence video micrographs of primary blast cells (c.l.ag. 40–45 hours) descended from an N teloblast injected with *tau::GFP* mRNA. The elapsed time (minutes) is indicated in the top right-hand corner of each panel. (A) Dividing *ns* cell. (B) Dividing *nf* cell. (C) A fortuitous specimen in which an *ns* and a younger *nf* cell (separated by a two-cell *nf* clone and an undivided *ns* cell) were dividing simultaneously. Broken outlines indicate the cell borders; arrows indicate the spindle midbody. Scale bar: 10  $\mu$ m.

mitosis. Cytokinesis occurred with the spindles displaced towards the posterior end of the cell, with the result that the cleavage furrow was also shifted posteriorly. The posterior shift of the spindle was correlated with a diminution in fluorescence of the posterior aster relative to the anterior aster in both cell types. The intensity difference between the anterior and posterior poles was not observed until after the completion of spindle rotation. Though we could not stain for DNA in these experiments, we estimate that the change in the posterior spindle pole occurred at the onset of anaphase. The posterior displacement of the furrow was greater in *nf* than in *ns* (Fig. 9C), as was the relative diminution of the posterior spindle pole fluorescence (Fig. 9B, 22–24 minutes). Within the *nf* blast cells, the spindle midbody was displaced towards the posterior centrosome, which further increased the extent of the mitotic asymmetry (Fig. 9C, 10 minutes). This difference between *nf* and *ns* correlates with the differences in the nuclear volume ratios of their respective progeny (Fig. 7).

## Discussion

### mRNA injections in *Helobdella*

Our results demonstrate the utility of routine mRNA injections for expressing cytoplasmic and nuclear localized versions of GFP and related fluorescent proteins, tau::GFP, and *lacZ* at readily detectable levels in *Helobdella* embryos without perturbing normal development. In situ hybridization revealed that the injected mRNAs are distributed throughout the cytoplasm of the injected teloblast and its blast cell progeny. Consistent with this, expressed proteins were seen in all progeny, in contrast to the mosaic expression seen when DNA is injected into teloblasts (data not shown) (Pilon and Weisblat, 1997). Some RNA injections give mosaic expression in *Xenopus* and *Danio* embryos (Sive et al., 2000; Geldmacher-Voss et al., 2003). We speculate that the slower cell divisions in leech may give time for the injected RNA to spread prior to cytokinesis.

Injected mRNA is degraded more quickly in the blast cells than in the teloblast, and more quickly within the germinal bands than in the bandlets. Previous work has shown that blast cells accumulate transcripts more rapidly than teloblasts (Bissen and Weisblat, 1991) and there is a dramatic prolongation of the cell cycle in blast cells relative to teloblasts (Zackson, 1984; Bissen and Weisblat, 1989). These features support the idea that the teloblast-to-blast cell transition in leech is analogous to the 'mid-blastula transition' in *Xenopus* and *Drosophila* (reviewed by Yasuda and Schubiger, 1992).

For all the mRNAs tested, we observed graded expression of the encoded protein; the first blast cells born after injection contain low levels of the protein and those born later contain progressively higher levels. No such gradient is observed when passive tracers are used. From the in situ results and the stem cell mode by which blast cells arise, we conclude that: (1) clones founded by blast cells born immediately after the injection contain only the relatively low levels of protein expressed before the mRNA they inherit from the teloblast is degraded; and (2) blast cells born at progressively later times post-injection inherit not only the mRNA, but also inherit increasing amounts of protein expressed in the teloblast, in which the injected message is relatively stable.

Whatever the mechanism by which they are formed, the gradients of protein expression driven by injection of synthetic mRNAs means that dose effects of mutant or ectopic regulatory and signaling proteins from such injections can be determined simply by examining their effects on blast cells born at different times and by comparing their effects on teloblast divisions at various times after injection (S.O.Z. and D.A.W., unpublished). Finally, we have demonstrated the efficacy and specificity of AS MO knockdown as a means of modulating the expression of injected mRNAs. Together, these techniques provide a powerful tool for functional analysis of gene function in an animal for which standard genetic approaches are not available.

### Application of the mRNA injection technique to analysis of the N teloblast lineage

In *Helobdella*, most ganglionic neurons arise from the N teloblasts via two distinct classes of blast cells, ns and nf, that arise in exact alternation. Homologous lineages have been described in both lumbricid and tubificid oligochaetes (Storey, 1989; Arai et al., 2001). Therefore, this grandparental mode of

stem cell division is almost certainly ancestral to clitellate annelids. To further understand this process, we have applied the mRNA injection technique in three ways.

(1) We used nGFP lineage tracer to extend our knowledge of the nf and ns blast cell lineages, and to ascertain the fates of the initial 'non-standard' early progeny of the N teloblasts. We find that the nf and ns lineages differ from one another in terms of timing, orientation and asymmetry of mitoses. Moreover, the nf lineage differs from ns in that the anterior cell at each of the first four divisions shows a markedly shorter cell cycle time than its posterior sister cell. As a result, the nf lineage shows a stem cell-like pattern. Similar division patterns, but with a more rapid time course, have been seen for a genetically distinct strain of *H. robusta* (F. Z. Huang, personal communication). Regarding the early progeny of the N teloblast, we find that the first cell born from the N teloblast undergoes symmetric and relatively rapid divisions. This cell, which we designate n°, generates a clone with no obvious homology to either nf or ns, and is predicted to contribute to the adhesive organ. The second cell born from the N teloblast gives rise to an nf-like clone. We predict that it contributes 'extra' N teloblast derivatives primarily to the most rostral of the segmental neuromeres (R1) in the subesophageal ganglion.

(2) Using the localized nGFP fluorescence, we quantified the nuclear volumes of the sister cells resulting from nf and ns divisions. The volume ratios ( $V_{nf,p}/V_{nf,a}$  and  $V_{ns,p}/V_{ns,a}$ ) varied only about 10% internally, and value for the nf progeny is less than half that for the ns progeny. These results indicate that the asymmetric divisions of nf and ns cell are under tight, differential control. Asymmetric cell divisions are a prominent feature of the stereotyped division patterns throughout the segmental and non-segmental tissues of the *Helobdella* embryo (Zackson, 1984; Shankland, 1987; Huang et al., 2002); we find that later divisions within the ns and nf blast cell lineages are also asymmetric. Whether such asymmetries are essential for establishing fate differences or merely a reflection of those differences remains to be determined. The most obvious way in which the stereotyped asymmetry (and/or orientation) of cell divisions could specify different fates for the progeny is by segregating asymmetrically localized fate determinants, as in the unequal first cleavage of the *Helobdella* embryo (Whitman, 1878; Astrow et al., 1987). Well studied examples include unequal division of the *C. elegans* zygote (Gotta and Ahringer, 2001) and *Drosophila* neuroblasts (Knoblich, 2001), as well as the asymmetric division of the *C. elegans* EMS cell that is induced by contact with blastomere P2 (Goldstein, 1995). Another effect of asymmetric cell divisions could be to position the progeny with respect to inductive influences of other cells, as seen in the EMS lineage of *C. elegans* (Goldstein, 1995). A third means by which an asymmetric cell division could influence cell fates would be by affecting the cell cycle duration and composition of the progeny. For example, the smaller posterior progeny of the n blast cells (nf.p and ns.p) have longer cell cycles than their siblings and the homologous cells in a congeneric species, *H. triserialis*, are the first cells in their lineage to go through a measurable G1 phase (Bissen and Weisblat, 1989). It seems likely that, in addition to accumulating 'housekeeping' transcripts and proteins required to progress through the cell cycle, these cells would also make different types of quantities of developmental regulatory gene

products as well. To our knowledge, no definitive example of this third possibility has been described.

(3) To pursue the mechanisms by which the asymmetric n blast cell divisions are controlled, we used tau::GFP fluorescence to follow n blast cell spindle dynamics. Centrosomes in the blast cells have separated well prior to the onset of mitosis. Spindles in the left n bandlet almost always rotate in a counterclockwise direction. The spindle is initially positioned symmetrically within the cell; the asters appear of equal size and fluorescence intensity until after rotation. Asymmetry emerges during late metaphase or anaphase, when the spindle moves posteriorly and the posterior aster undergoes a dramatic reduction in size/fluorescence intensity. We interpret this to mean that the astral microtubules of the anterior spindle pole are longer and/or more stable than those of the posterior pole. Finally, at least in the nf blast cells, a further degree of asymmetry is contributed by the posterior shift of the spindle midbody relative to the spindle poles.

In *C. elegans*, the asymmetric division of the zygote is driven by a posterior shift in the mitotic spindle (Albertson, 1984). By contrast, it has been reported that the asymmetric divisions of *Drosophila* neuroblasts involve a basal shift of the spindle midbody relative to the spindle poles (Kaltschmidt et al., 2000). Our findings show that these processes can occur together in cells, and that they can be regulated differentially to generate the distinct asymmetries of the alternating nf and ns blast cells in *Helobdella*.

We are indebted to Yanzhen Cui and Richard Harland for providing plasmids and for helpful discussions, which are crucial to the success of this work. We thank Françoise Huang, Sara Agee, Shirley Bissen, Marty Shankland and members of our laboratory for technical assistance and discussions; and Holly Aaron (Berkeley Molecular Imaging Center) and Steve Ruzin (CNR Biological Imaging Center) for assistance and training in confocal microscopy. This work was supported by NIH grant RO1 GM60240 to D.A.W. and by UC Regents Fellowship to S.O.Z.

## References

- Albertson, D. G. (1984). Formation of the first cleavage spindle in nematode embryos. *Dev. Biol.* **101**, 61-72.
- Amsterdam, A., Lin, S. and Hopkins, N. (1995). The *Aequorea victoria* green fluorescent protein can be used as a reporter in live zebrafish embryos. *Dev. Biol.* **171**, 123-129.
- Arai, A., Nakamoto, A. and Shimizu, T. (2001). Specification of ectodermal teloblast lineages in embryos of the oligochaete annelid *Tubifex*: involvement of novel cell-cell interactions. *Development* **128**, 1211-1219.
- Astrow, S. H., Holton, B. and Weisblat, D. A. (1987). Centrifugation redistributes factors determining cleavage patterns in leech embryos. *Dev. Biol.* **120**, 270-283.
- Bissen, S. T. and Weisblat, D. A. (1987). Early differences between alternate n blast cells in leech embryo. *J. Neurobiol.* **18**, 251-270.
- Bissen, S. T. and Weisblat, D. A. (1989). The duration and compositions of cell cycles in embryos of the leech, *Helobdella triserialis*. *Development* **106**, 105-118.
- Bissen, S. T. and Weisblat, D. A. (1991). Transcription in leech: mRNA synthesis is required for early cleavages in *Helobdella* embryos. *Dev. Biol.* **146**, 12-23.
- Braun, J. and Stent, G. S. (1989). Axon outgrowth along segmental nerves in the leech. I. Identification of candidate guidance cells. *Dev. Biol.* **132**, 471-485.
- Chalfie, M., Tu, Y., Euskirchen, G., Ward, W. W. and Prasher, D. C. (1994). Green fluorescent protein as a marker for gene expression. *Science* **263**, 802-805.
- Feng, G., Mellor, R. H., Bernstein, M., Keller-Peck, C., Nguyen, Q. T., Wallace, M., Nerbonne, J. M., Lichtman, J. W. and Sanes, J. R. (2000). Imaging neuronal subsets in transgenic mice expressing multiple spectral variants of GFP. *Neuron* **28**, 41-51.
- García-Bellido, A., Ripoll, P. and Morata, G. (1973). Developmental compartmentalisation of the wing disk of *Drosophila*. *Nat. New Biol.* **245**, 251-253.
- Geldmacher-Voss, B., Reugels, A. M., Pauls, S. and Campos-Ortega, J. A. (2003). A 90-degree rotation of the mitotic spindle changes the orientation of mitoses of zebrafish neuroepithelial cells. *Development* **130**, 3767-3780.
- Gimlich, R. L. and Braun, J. (1985). Improved fluorescent compounds for tracing cell lineage. *Dev. Biol.* **109**, 509-514.
- Gleizer, L. and Stent, G. S. (1993). Developmental origin of segmental identity in the leech mesoderm. *Development* **117**, 177-189.
- Goldstein, B. (1995). Cell contacts orient some cell division axes in the *Caenorhabditis elegans* embryo. *J. Cell Biol.* **129**, 1071-1080.
- Gotta, M. and Ahringer, J. (2001). Axis determination in *C. elegans*: initiating and transducing polarity. *Curr. Opin. Dev. Biol.* **11**, 367-373.
- Grill, S. W., Gonczy, P., Stelzer, E. H. and Hyman, A. A. (2001). Polarity controls forces governing asymmetric spindle positioning in the *Caenorhabditis elegans* embryo. *Nature* **409**, 630-633.
- Huang, F. Z., Kang, D., Ramirez-Weber, F. A., Bissen, S. T. and Weisblat, D. A. (2002). Micromere lineages in the glossiphoniid leech *Helobdella*. *Development* **129**, 719-732.
- Hyman, A. A. (1989). Centrosome movement in the early divisions of *Caenorhabditis elegans*: a cortical site determining centrosome position. *J. Cell Biol.* **109**, 1185-1193.
- Kaltschmidt, J. A., Davidson, C. M., Brown, N. H. and Brand, A. H. (2000). Rotation and asymmetry of the mitotic spindle direct asymmetric cell division in the developing central nervous system. *Nat. Cell Biol.* **2**, 7-12.
- Knoblich, J. A. (2001). Asymmetric cell division during animal development. *Nat. Rev. Mol. Cell Biol.* **2**, 11-20.
- Kramer, A. P. and Weisblat, D. A. (1985). Neural kinship groups in the leech. *J. Neurosci.* **5**, 388-407.
- Kuo, D. H. and Shankland, M. (2004). Evolutionary diversification of specification mechanisms within the O/P equivalence group of the leech genus *Helobdella*. *Development* **131**, 5859-5869.
- Lee, T. and Luo, L. (1999). Mosaic analysis with a repressible cell marker for studies of gene function in neuronal morphogenesis. *Neuron* **22**, 451-461.
- Lent, C. M., Zundel, D., Freedman, E. and Groome, J. R. (1991). Serotonin in the leech central nervous system: anatomical correlates and behavioral effects. *J. Comp. Physiol. (A)*. **168**, 191-200.
- Lippincott-Schwartz, J. and Patterson, G. H. (2003). Development and use of fluorescent protein markers in living cells. *Science* **300**, 87-91.
- Liu, N.-J. L., Isaksen, D. E., Smith, C. M. and Weisblat, D. A. (1998). Movements and stepwise fusion of endodermal precursor cells in leech. *Dev. Genes Evol.* **208**, 117-127.
- Martindale, M. Q. and Shankland, M. (1990). Intrinsic segmental identity of segmental founder cells of the leech embryo. *Nature* **347**, 672-674.
- Muller, K. J., Nicholls, J. G. and Stent, G. S. (1981). *Neurobiology of the Leech*. Cold Spring Harbor, NY: Cold Spring Harbor Laboratory Press
- Nardelli-Haeffiger, D., Bruce, A. E. E. and Shankland, M. (1994). An axial domain of HOM/Hox gene expression is formed by morphogenetic alignment of independently specified cell lineages in the leech *Helobdella*. *Development* **120**, 1839-1849.
- Pilon, M. and Weisblat, D. A. (1997). A *nanos* homolog in leech. *Development* **124**, 1771-1780.
- Sandig, M. and Dohle, W. (1988). The cleavage pattern in the leech *Theromyzon tessulatum* (Hirudinea, Glossiphoniidae). *J. Morphol.* **196**, 217-252.
- Seaver, E. C. and Shankland, M. (2000). Leech segmental repeats develop normally in the absence of signals from either anterior or posterior segments. *Dev. Biol.* **224**, 339-353.
- Shain, D. H., Ramirez-Weber, F. A., Hsu, J. and Weisblat, D. A. (1998). Gangliogenesis in leech: morphogenetic processes leading to segmentation in the central nervous system. *Dev. Genes Evol.* **208**, 28-36.
- Shain, D. H., Stuart, D. K., Huang, F. Z. and Weisblat, D. A. (2000). Segmentation of the central nervous system in leech. *Development* **127**, 735-744.
- Shankland, M. (1987). Differentiation of the O and P cell lines in the embryo of the leech. II. Genealogical relationship of descendant pattern elements in alternative developmental pathways. *Dev. Biol.* **123**, 97-107.
- Shankland, M., Bissen, S. T. and Weisblat, D. A. (1992). Description of the California leech *Helobdella robusta* nov. sp., and comparison to *H.*

- triserialis* on the basis of morphology, embryology, and experimental breeding. *Can. J. Zool.* **70**, 1258-1263.
- Sive, H. L., Grainger, R. M. and Harland, R. M.** (2000). *Early Development of Xenopus laevis: A Laboratory Manual*. Cold Spring Harbor, NY: Cold Spring Harbor Laboratory Press.
- Smith, C. M. and Weisblat, D. A.** (1994). Micromere fate maps in leech embryos: lineage-specific differences in rates of cell proliferation. *Development* **120**, 3427-3438.
- Song, M. H., Huang, F. Z., Chang, G. Y. and Weisblat, D. A.** (2002). Expression and function of an *even-skipped* homolog in the leech *Helobdella robusta*. *Development* **129**, 3681-3692.
- Storey, K. G.** (1989). Cell lineage and pattern formation in the earthworm embryo. *Development* **107**, 519-532.
- Torrence, S. A. and Stuart, D. K.** (1986). Gangliogenesis in leech embryos: migration of neural precursor cells. *J. Neurosci.* **6**, 2736-2746.
- Tsien, R. Y.** (1998). The green fluorescent protein. *Annu. Rev. Biochem.* **67**, 509-544.
- Tsubokawa, R. and Wedeen, C. J.** (1999). Cell death in late embryogenesis of the leech *Helobdella*. *Dev. Genes Evol.* **209**, 515-525.
- Weisblat, D. A. and Shankland, M.** (1985). Cell lineage and segmentation in the leech. *Philos. Trans. R. Soc. Lond. Ser. B.* **312**, 39-56.
- Weisblat, D. A. and Huang, F. Z.** (2001). An overview of glossiphoniid leech development. *Can. J. Zool.* **79**, 218-232.
- Weisblat, D. A., Zackson, S. L., Blair, S. S. and Young, J. D.** (1980). Cell lineage analysis by intracellular injection of fluorescent tracers. *Science* **209**, 1538-1541.
- Whitman, C. O.** (1878). The embryology of *Clepsine*. *Q. J. Microsc. Sci.* **18**, 215-315.
- Yasuda, G. K. and Schubiger, G.** (1992). Temporal regulation in the early embryo: is MBT too good to be true? *Trends Genet.* **8**, 124-127.
- Zackson, S. L.** (1982). Cell clones and segmentation in leech development. *Cell* **31**, 761-770.
- Zackson, S. L.** (1984). Cell lineage, cell-cell interaction, and segment formation in the ectoderm of a glossiphoniid leech embryo. *Dev. Biol.* **104**, 143-160.